Eur Biophys J
DOI 10.1007/s00249-015-1047-4

ORIGINAL PAPER

EBSA
Biophysics in Europe

Steered molecular dynamics approach for promising drugs for influenza A virus targeting M2 channel proteins

Hung Nguyen[1] · **Ly Le**[1,2]

Received: 29 December 2014 / Revised: 20 April 2015 / Accepted: 14 May 2015

Abstract We have used steered molecular dynamics simulation to investigate the molecular interactions between four M2 inhibitors (amantadine, rimantadine, and two other amantadine derivatives) and the M2 protein channels of influenza A virus H5N1, including the wild type (WT) and three previously identified drug-resistant variants (G34A, S31N, and V27A). The binding free energies between these four inhibitors and the M2 channel of the WT and the three mutants were also determined by use of the molecular mechanics–Poisson–Boltzmann surface area method. Our study provides important insight into binding affinity, including detailed energy components and interactions at the molecular level of four potential inhibitors with the M2 channel of drug-resistant strains; this may assist further experimental study and strategies for rational design of new inhibitors.

Keywords Influenza A virus · M2 channel proteins · Drugs A1 (amantadine), A2 (rimantadine), A3, and A4 · Wild type, G34A, S31N, and V27A mutants · Binding energy · Drug design

Electronic supplementary material The online version of this article (doi:10.1007/s00249-015-1047-4) contains supplementary material, which is available to authorized users.

✉ Ly Le
ly.le@hcmiu.edu.vn

Hung Nguyen
hung.nv@icst.org.vn

[1] Life Science Laboratory, Institute for Computational Science and Technology, Ho Chi Minh City, Vietnam

[2] School of Biotechnology, Ho Chi Minh City International University, Ho Chi Minh City, Vietnam

Introduction

The influenza A M2 channel protein is regarded as an important target in anti-influenza drug design because of its importance in viral infection (Holsinger and Lamb 1991; Sugrue and Hay 1991; Takeda et al. 2002). The tetrameric structure of M2 protein forms a pH-dependent channel through the viral membrane which controls proton conductance when the virus penetrates infected cells (Pinto et al. 1992; Pielak and Chou 2010; Lin and Schroeder 2001). Acidification weakens electrostatic interactions between matrix proteins and ribonucleoprotein (RNP) complexes, causing disintegration of the viral membrane and release of uncoated RNPs into the cytosol for transportation to the nucleus. Because of its crucial importance in influenza viral pathogenesis, to enable structure-based drug development a variety of structures of the M2 channel have been solved (Tran et al. 2013) by use of different techniques, for example site-directed infrared dichroism (Kukol et al. 1999), UV resonance Raman spectroscopy (Okada et al. 2001), electron spin resonance spectroscopy, and solid-state nuclear magnetic resonance (NMR) spectroscopy (Nishimura et al. 2002; Kovacs et al. 2000; Tian et al. 2003; Schnell and Chou 2008).

The M2 channel has four identical subunits (monomers) each of which contains 97 residues (Lamb et al. 1985) and comprises three main segments: an extracellular N-terminal segment (residues 1–23), a transmembrane (TM) segment (residues 24–46), and an intracellular C-terminal segment (residues 47–97) (Pielak and Chou 2010). The transmembrane (TM) segment is the main region responsible for proton conduction and is important in the search for a means of inhibition of the channel. Hence, to investigate proton conductance of M2 channel proteins for drug development, the primarily focus should be on this segment (Nishimura

Published online: 02 June 2015

et al. 2002; Hu et al. 2007; Stouffer et al. 2008; Cady and Hong 2008; Cady et al. 2010; Acharya et al. 2010). Residues 24–46 of the four monomers form a TM helix bundle lined by polar residues (Val27, Ser31, Gly34, His37, Trp41, Asp44, and Arg45). The tetrameric His37–Trp41 cluster is at the center of acid activation and proton conductance (Tang et al. 2002; Venkataraman et al. 2005; Hu et al. 2006). The ionizable His37 is essential for proton selectivity and acts as a channel sensor (Wang et al. 1995). Trp41 is important for unidirectional conductance and acts as a proton gate (Pielak and Chou 2010; Tang et al. 2002). It has recently been proposed that Val27 forms a secondary gate with His37 (Yi et al. 2008).

Some M2 inhibitors have been approved by the FDA. 1-Aminoadamantane hydrochloride (A1), also known as amantadine, is the first efficient drug in influenza therapeutics. A1 indirectly inhibits virus activity by using a hydrophobic cage to prevent proton conduction by the ion-channel. Another drug approved for treating influenza A, A2 (rimantadine; α-methyl-1-adamantane methylamine hydrochloride), has efficacy comparable with that of A1 but is of greater risk because of adverse effects (Stephenson and Nicholson 2001; Jefferson et al. 2004). However, A1 and A2 are currently under restricted application and not recommended for influenza A treatment by the WHO because of the rapid occurrence of drug resistance. To inhibit the M2 proton channel, new inhibitors have been designed to fight influenza A epidemics. Amantadine derivatives A3 and A4 have been proposed as potential candidates for M2 proton channel inhibition in further studies (Tran et al. 2011; Le and Leluk 2011; Tran and Le 2014).

The binding sites of A1 and A2 on the M2 channel have been a controversial issue for more than twenty years. They have been predicted on the basis of the location of drug-resistant mutations at residues 26, 27, 30, 31, 34, and 38 (Hay et al. 1985; Wang et al. 1993). Interestingly, it has been predicted that the side chains of amino acids 27, 31, and 34 face the channel interior, leading to the hypothesis that the drugs bind the inside of the channel (Pielak and Chou 2010). Schnell and Chou (2008), however, by use of nuclear Overhauser effect (NOE) experiments, detected four equivalent binding sites of A2 outside the channel. They suggested that, by binding at a lipid-facing pocket formed by Trp41, Ile42, and Arg45 from one TM helix and Leu40, Leu43, Asp44 from the adjacent TM helix, A2 acts as a link between two adjoining helixes and indirectly keeps the channel gate closed. A recent study has also suggested that binding of amantadine and its derivatives at positions inside the M2 channel is more energetically favorable (Jing et al. 2008; Ohigashi et al. 2009). For this reason, complexes which have the drugs binding inside the channel should be used for further investigation.

The purpose of our research was to investigate, by use of steered molecular dynamics (SMD) simulation, the binding pathway of known drugs and new candidates (A1, A2, and two A2 derivatives) within M2 protein channels, to gain insight into the mechanism of how points of mutation lead to drug resistance. Specifically, we conducted the simulation for four inhibitors in complexes with four M2 protein channels including that of H5N1 wild-type (WT), and three other drug-resistant mutants (G34A, S31N, and V27A).

Materials and methods

Materials

The 3D structure of the M2 channel was taken from the Protein Data Bank (PDB entry 2L0J, strain A/Udon/307/1972); this was derived from a complex embedded in DMPC liposomes (Sharma et al. 2010). The lipid membrane was used as the model membrane of the DOPC bilayer; it contained 128 lipid molecules (52 per leaflet) (Klösgen and Helfrich 1997). The A1 drug coordinate was extracted from complex 3C9J, and the A2, A3, and A4 drug structures were constructed on the basis of the A1 structure by use of GaussView 5.0. The geometries of all four drugs were then optimized by use of Gaussian 09 (Fig. 1) (Frisch et al. 2004).The G34A, S31N, and V27A mutant models were generated by use of the mutagenesis tool of the software Visual Molecular Dynamics (VMD) (Humphrey et al. 1996); these mutants were then energy-minimized by use of 500,000 steps of the steepest descent minimization algorithm of the GROMACS 4.5.5 package (Hess et al. 2008). AutoDock Vina software (Trott and Olson 2010) was then used to identify the site of binding of the drugs to the M2 channel, before SMD simulation as follows:

- *Structure preparation* Several modifications of the original protein and drug structures were made by using different software to facilitate molecular docking. VMD was used to visualize and separate the receptor for docking. Auto-dock tools (ADT) were used to convert pdb files to pdbqt files for the docking process. All ligands and proteins in the pdb format were converted to the pdbqt format with correction of charges for docking.
- *Molecular docking* The docking procedure requires identification of the binding box position, which is the active site of the protein. This was achieved by use of the crystal structure of the protein with bound inhibitors. The grid box for protein–ligand docking was designed to fit the protein surface.
- *Analysis of the results* The docking results were analyzed and ranked by lowest binding energy and RMS deviation. The results indicate high-affinity binding

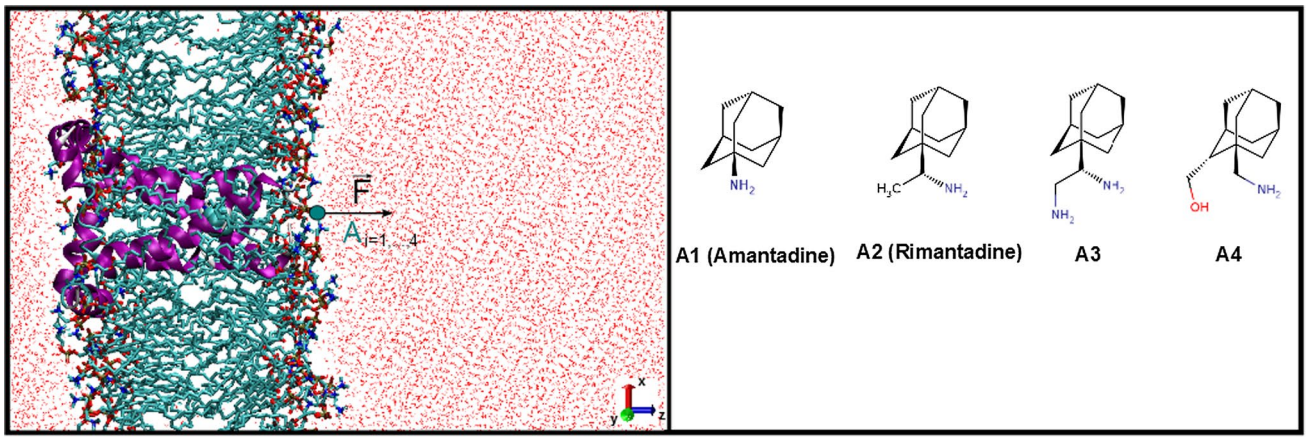

Fig. 1 Direction of SMD for the M2 proton channel (*left*) and the four inhibitor structures (*right*)

sites and possible active site interaction. The binding conformations of drug molecules with the protein were analyzed to reveal the basic interactions and to characterize possible active site-related residues responsible for binding, by use of VMD software.

Steered molecular dynamics (SMD) method

The GROMACS 4.5.5 package (Hess et al. 2008) was used to run MD simulations with the GROMOS96 force field (van Gunsteren et al. 1996). The electrostatic and vdW interactions were set at 1.4 and 1.2 nm cut-off (the same value was not chosen for both electrostatic and vdW interactions because the electrostatic interaction has a longer-range effect than the van der Waals interaction). The electrostatic interaction was calculated by use of the particle-mesh Ewald summation method (Darden et al. 1993). The complex was solvated in the SPC water model (Mark and Nilsson 2001); it was placed in a triclinic box with edges of 6.6, 6.4, and 12.0 nm; the center of the protein was placed at 3.3, 3.2, and 2.5 nm. The equilibration process was performed with coupling with temperature and pressure conditions. A constant temperature of 310 K was enforced by use of the Berendsen algorithm (Berendsen et al. 1984) under 500 ps for constant volume and temperature (NVT); Parrinello–Rahman pressure coupling (Parrinello and Rahman 1981) in 500 ps for constant pressure and temperature (NPT) was run at 1 bar constant pressure. All bond lengths were constrained with the linear constraint solver LINCS (Hess et al. 1997) as implemented in the GROMACS package. We tried pulling with speed $v = 0.005$ nm/ps, and the spring constant was chosen as $k \approx 1020$ pN/nm. Pulling in the z direction was used for all complexes, and SMD runs of 1000 ps were needed to entirely move the drug from the M2 channel. Molecular dynamics simulations enabled integration of the equations of motion with time steps of 2 fs in the leap-frog algorithm (Hockney et al. 1974).

MM-PBSA method

Binding free energies between drugs A1, A2, A3, and A4 and the M2 channel of the WT and three mutants were calculated by use of the molecular mechanics–Poisson–Boltzmann surface area (MM-PBSA) method (Wang et al. 2001; Nguyen et al. 2011).

Results and discussion

Steered molecular dynamics (SMD) simulation was used to study the mechanism of binding of the four inhibitors (A1, A2, and the two A2 derivatives), and the effect of three drug-resistant mutations (G34A, S31N, and V27A) on the binding pocket of the M2 channel of the WT and the three mutants. The simulation process was conducted to pull the drugs from the stably bound position inside the M2 channels and to estimate the energy needed for this process.

The maximum pulling force F_{max} is required to break hydrogen bonds between the drugs and the M2 channel and to move the drugs from the M2 channel binding pocket. The time from the starting point to F_{max} is the time taken to pull drug from the stably bound to the unbound position (Le et al. 2010). The pulling force profiles during the process of steering drugs A1, A2, A3, and A4 from the binding pocket were followed as shown in Fig. 2. Details of F_{max} and the docking scores for the inhibitors of the M2 channel are shown in Table S1 (supporting information). For the WT structure (Fig. 2a), the time taken to pull A3 (at F_{max} 477.206 pN) and A4 (at F_{max} 526.331 pN) out of the M2 channel reached a value of approximately 200 ps; values for A1 (at F_{max} 453.922 pN)

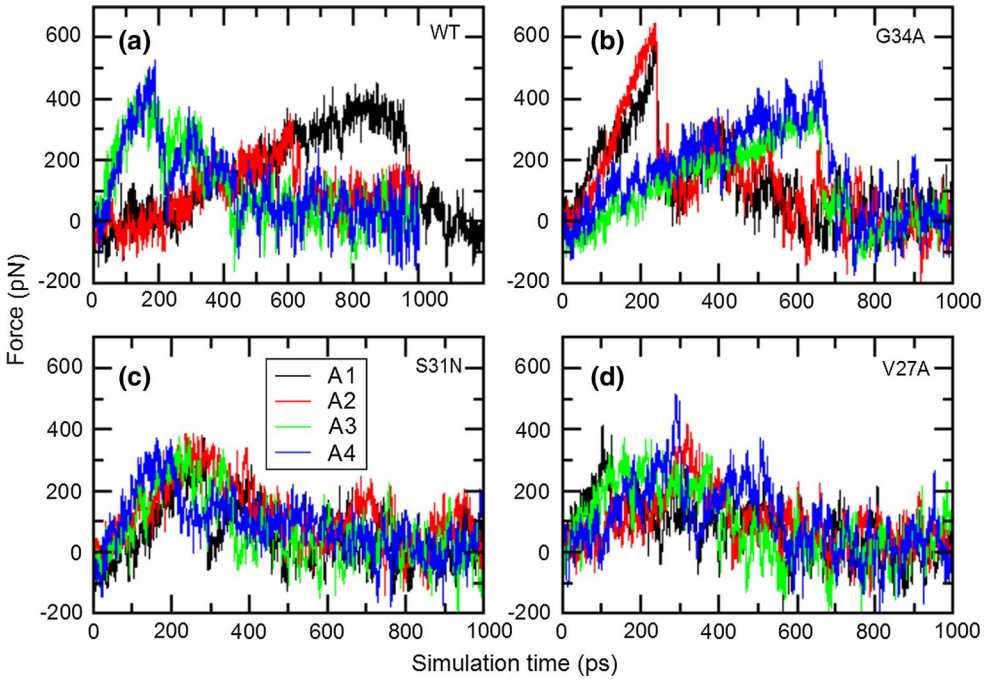

Fig. 2 Pulling force profiles for drugs A1, A2, A3, and A4 binding to the M2 channel of the WT (**a**), and mutants G34A (**b**), S31N (**c**), and V27A (**d**)

and A2 (at F_{max} 354.202 pN) were approximately 1000 ps and approximately 600 ps, respectively. Briefly, with the same starting pulling force, A3 and A4 were seen to leave the binding pocket of the M2 channel sooner than A1 and A2. This suggests that the two FDA-approved drugs A1 and A2 are more potent inhibitors of the M2 channel of WT H5N2 than the newly modified candidates A3 and A4. In contrast with the WT, for the mutant G34A (Fig. 2b) the times taken to pull the drugs from the M2 channel were approximately 250 ps for A1 (at F_{max} 579.902 pN) and A2 (at F_{max} 647.058 pN) and approximately 700 ps for A3 (at F_{max} 375.490 pN) and A4 (at F_{max} 524.930 pN). Therefore, A1 and A2 are more easily pulled from the binding pocket of the mutant G34A and their complexes are less stable than those of A3 and A4. This means the G34A mutation is important in binding of the drugs to the M2 channel. Figure 2c, d show the pulling force profiles for mutants S31N and V27A. For mutant S31N (Fig. 2c), the pulling time is approximately 250 ps for A1 (at F_{max} 376.050 pN), A2 (at F_{max} 388.235 pN), A3 (at F_{max} 377.311 pN), and A4 (at F_{max} 374.510 pN). Similar to mutant V27A (Fig. 2d), the time needed to pull the drugs from the M2 channel reach a value of approximately 150 ps for A1 (at F_{max} 413.725 pN) and A3 (at F_{max} 373.109 pN), and approximately 350 ps for A2 (at F_{max} 420.728 pN) and A4 (at F_{max} 511.971 pN). So, there are no significant differences between the complexes of the drugs for these two mutants. Different from the WT and G34A, all four inhibitors were found to leave the binding pocket quickly under the effect of the same initial steering force for mutants S31N and V27A.

Interaction energy (including electrostatic and vdW interactions) between the four drugs and the M2 channel for the WT and the three mutants G34A, S31N, and V27A, shown in Fig. 3, is in good agreement with pulling force profiles. At 0 ps, the interaction energies between A3 and A4 and the WT M2 channel were lower than those for A1 and A2 (Fig. 3a). The interaction energies of A3 and A4 with the M2 channel reached 0 kcal/mol at approximately 250 ps, which is much faster than for A1 (approx. 1000 ps) and A2 (approx. 650 ps). For mutant G34A (Fig. 3b), the interaction energies between the drugs and the M2 channel reach 0 kcal/mol at approximately 375 ps for A1 and A2, which is much faster than for A3, approximately 1000 ps, and for A4, approximately 850 ps. This means that for A1 and A2 the interaction energy between the drugs and the M2 channel reached approximately 0 kcal/mol more quickly than for A3 and A4. Thus, the interaction energy profiles confirm that the G34A mutation is important in the interaction between the drugs and the M2 channel. The effect of changing the interaction energies of the drugs with the M2 proton channels of mutants S31N and V27A are shown in Fig. 3c, d. For mutant S31N the interaction energy makes a small difference. In particular, the interaction energies of drugs A1 and A3 reach 0 kcal/mol after 250 ps; that for A2 reaches 0 kcal/mol after 600 ps and that for A4 reaches 0 kcal/mol after 375 ps. For the V27A mutant, the interaction energy between the M2 channel and all four drugs reaches 0 kcal/mol after 400 ps. Here, there are no significant differences between the interaction energies for mutants S31N and V27A. Compared with the WT, the three mutated residues lead to significant changes in

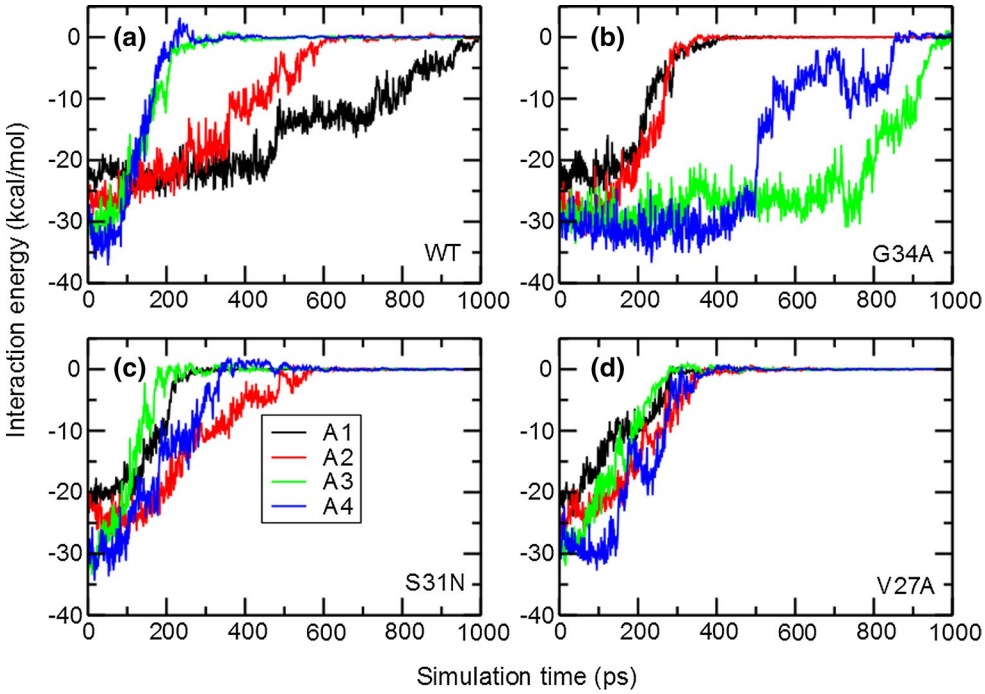

Fig. 3 Interaction energy between drugs A1, A2, A3, and A4 and the M2 channel for the WT (**a**), and for the mutants G34A (**b**), S31N (**c**), and V27A (**d**) as a function of time

the interaction energy between the M2 channel and these drugs.

To determine the effect of mutated residues on interactions between the drugs and the M2 channel proteins at the active site at a molecular level, we showed all hydrogen bond and hydrophobic interactions by use of LigPlot software (Wallace et al. 1995; Roman and Swindells 2011) (Fig. 4). We found that:

1. for the WT, residues Val27, Ala30, Ser31, and Gly34 were forming hydrogen bonds with A1, A2, A3, and A4 in the binding pocket, and the Ser31 residue bound strongly with all four drugs;
2. for mutant G34A, loss of a hydrogen bond with the binding site residues, because of the effect of a mutated residue, was observed for A1 and A2 but not for A3 and A4, which is consistent with the high potency of these two drugs;
3. for mutant S31N, the S31N residue was not seen to bind directly to A1, A2, and A3 but it did bind to A4
4. for mutant V27A, the V27A residue was seen to form a hydrogen bond with A1, A2, and A3, but not with A4; mutation V27A stays close to the drugs but is, in general, not a significant mutation because valine and alanine are chemically similar.

To gain insight into the contribution of each energy component to drugs' potency, the binding free energies between the four drugs and the M2 channel of the WT and the three mutants were calculated by use of the MM-PBSA method; the results are shown in Table 1.

In all the simulated complexes, electrostatic interactions, apolar solvation, and polar solvation made no significant distribution to binding free energy differences when the four drugs were compared. The vdW interaction and entropy, however, are of major importance to the free energy of binding between the drugs and the M2 channel proteins. In the WT, the entropy ($-T\Delta S$) of the complexes fluctuated around -14 kcal/mol for all the drugs, revealing that the entropy does not make crucial contributions to the differences between the binding free energies of these complexes. In contrast, however, the vdW interaction between receptor and drugs is -20.910 kcal/mol for A1, -24.448 kcal/mol for A2, -4.028 kcal/mol for A3, and -4.354 kcal/mol for A4; this indicates that the different free energies for binding between A1, A2, A3, and A4 and the M2 channel are caused mainly by the vdW interaction. The binding free energies for A1 (-30.741 kcal/mol) and A2 (-34.585 kcal/mol) were much smaller than those for A3 (-17.431 kcal/mol) and A4 (-17.194 kcal/mol). Our results are in good agreement with previous experimental results which revealed that A1 and A2 strongly inhibit the activity of the M2 channel (Du et al. 2010). For mutant G34A, the entropy values of the complexes are significantly different. In detail, the entropies of the complexes are $-T\Delta S = -16.579$ kcal/mol for A1, $-T\Delta S = -7.348$ kcal/mol for A2, $-T\Delta S = -39.353$ kcal/mol for A3, and $-T\Delta S = -39.597$ kcal/mol for A4. Therefore, the entropies of the complexes of A3 and A4 were

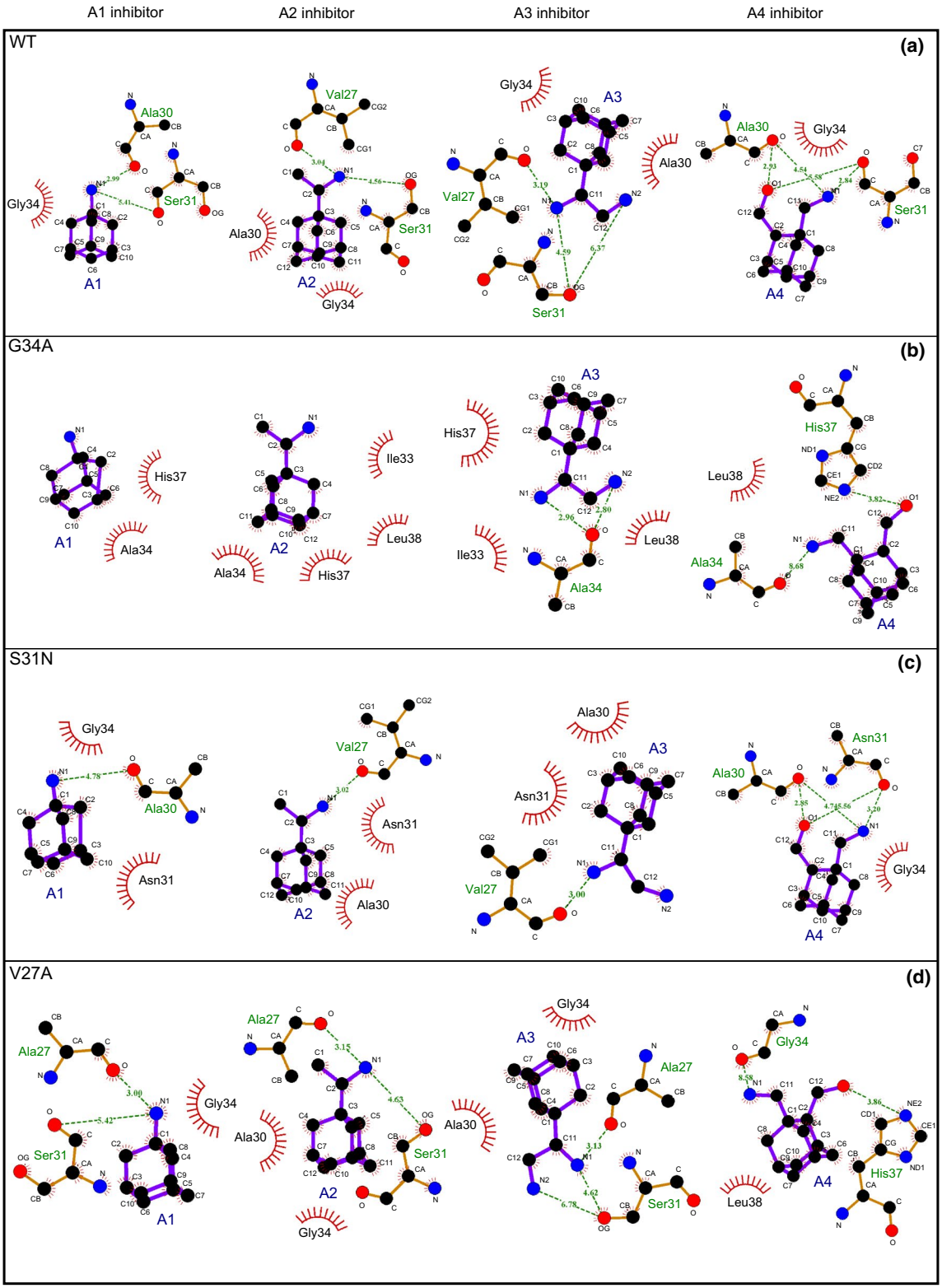

Fig. 4 Hydrogen bonding and hydrophobic interactions between A1, A2, A3, and A4 and the M2 channel of the WT (**a**), and mutants G34A (**b**), S31N (**c**) and 27A (**d**). The figure was prepared by use of LigPlot software (Wallace et al. 1995; Roman and Swindells 2011)

Table 1 Binding free energies (kcal/mol) between the drugs and the M2 channel protein of the WT and the three mutants, calculated by use of the MM-PBSA method

	ΔE_{elec}	ΔE_{vdW}	ΔG_{apolar}	ΔG_{polar}	$-T\Delta S$	ΔG_{bind}
Wild type						
A1	0.018 ± 0.013	-20.910 ± 3.119	-0.151 ± 0.014	4.991 ± 1.157	-14.689 ± 1.932	-30.741 ± 4.317
A2	0.782 ± 0.015	-24.448 ± 2.702	-0.179 ± 0.017	3.974 ± 0.713	-14.714 ± 2.003	-34.585 ± 3.904
A3	-0.556 ± 0.027	-4.028 ± 1.897	-0.065 ± 0.009	1.398 ± 0.370	-14.180 ± 2.417	-17.431 ± 2.538
A4	-0.138 ± 0.016	-4.354 ± 1.672	-0.063 ± 0.005	1.739 ± 0.283	-14.378 ± 2.301	-17.194 ± 1.912
G34A mutant						
A1	-0.035 ± 0.022	-5.405 ± 1.452	-0.089 ± 0.007	1.305 ± 0.011	-16.579 ± 2.101	-20.803 ± 3.371
A2	-0.165 ± 0.013	-6.125 ± 1.431	-0.094 ± 0.003	2.293 ± 0.114	-7.348 ± 1.107	-11.439 ± 1.426
A3	0.815 ± 0.032	-24.523 ± 3.133	-0.483 ± 0.035	3.784 ± 0.233	-39.353 ± 5.212	-59.760 ± 4.887
A4	-0.746 ± 0.029	-17.309 ± 2.016	-0.352 ± 0.011	4.162 ± 0.772	-39.597 ± 3.593	-53.842 ± 5.171
S31N mutant						
A1	-0.034 ± 0.003	-3.583 ± 0.997	-0.062 ± 0.005	1.299 ± 0.078	-7.865 ± 1.210	-10.245 ± 1.703
A2	0.009 ± 0.002	-7.125 ± 1.413	-0.119 ± 0.023	2.602 ± 0.716	-16.033 ± 2.877	-20.666 ± 2.978
A3	-0.273 ± 0.011	-3.354 ± 1.171	-0.057 ± 0.002	1.943 ± 0.331	-16.384 ± 2.071	-18.125 ± 2.336
A4	0.026 ± 0.003	-6.014 ± 1.733	-0.091 ± 0.010	2.252 ± 0.431	-7.808 ± 1.719	-11.635 ± 1.221
V27A mutant						
A1	0.028 ± 0.017	-3.587 ± 0.856	-0.066 ± 0.010	1.447 ± 0.122	-14.575 ± 2.130	-16.753 ± 2.775
A2	0.087 ± 0.025	-5.509 ± 1.211	-0.091 ± 0.017	2.036 ± 0.787	-14.545 ± 1.839	-18.022 ± 2.471
A3	-0.362 ± 0.073	-4.003 ± 0.444	-0.073 ± 0.018	1.693 ± 0.301	-7.260 ± 0.975	-10.005 ± 1.102
A4	-0.426 ± 0.033	-6.112 ± 1.229	-0.097 ± 0.008	2.512 ± 1.079	-7.339 ± 1.103	-11.462 ± 2.178

smaller than those of the complexes of A1 and A2. This means the positions of complexes of A3 and A4 in the active site of mutant G34A varied substantially. In addition, the vdW interactions between the drugs and the receptor are also very different for the four complexes—−5.405 kcal/mol for A1, −6.125 kcal/mol for A2, −24.523 kcal/mol for A3, and −17.309 kcal/mol for A4. The differences for both entropy and vdW interactions among the complexes leads to the different binding free energies between the drugs and M2 channel for mutant G34A. As a result, the binding free energies for A3 (−59.760 kcal/mol) and A4 (−53.842 kcal/mol) were much smaller than those for A1 (−20.803 kcal/mol) and A2 (−11.439 kcal/mol). That A3 and A4 were found to bind more strongly than A1 and A2 to the M2 channel by MM-PBSA calculations is in good agreement with the SMD result. Similar to the WT and mutant G34A, the entropy and vdW interactions for mutants S31N and V27A are also crucial to the different binding free energies between the drugs and receptor. For mutant S31N, the binding free energies for A2 (−20.666 kcal/mol) and A3 (−18.125 kcal/mol) are smaller than those for A1 (−10.245 kcal/mol) and A4 (−11.635 kcal/mol). A2 and A3 have greater affinity for the M2 channel than A1 and A4. For mutant V27A, A1 and A2 have greater binding affinity for the M2 channel than A3 and A4. The binding free energies for A1 (−16.753 kcal/mol) and A2 (−18.022 kcal/mol) are smaller than those for A3 (−10.005 kcal/mol) and A4 (−11.462 kcal/mol). The different binding energies for mutant V27A are highly similar to the results for the WT, which is reasonable because valine and alanine are chemically similar.

Conclusions

By using SMD simulation to study the mechanism of binding of four inhibitors (A1, A2, A3, and A4) to influenza A M2 channel proteins, including the wild-type and three mutants (V27A, S31N, G34A), we made the major discovery that drugs A1 and A2 bind strongly to influenza A virus wild-type M2 and to mutant V27A but may not bind efficiently to mutant G34A because of loss of hydrogen bonds, possibly as a result of the point of mutation. However, the reverse effect was observed for inhibitors A3 and A4. For mutant S31N, inhibitors A2 and A3 bound more effectively than A1 and A4. Our MM-PBSA results were not only in good agreement with experimental and SMD results but also revealed that the vdW interaction and entropy contribute substantially to the binding energy of the interaction between the inhibitors and the influenza A M2 proteins, in contrast with electrostatic interactions, and polar and apolar solvation. Our study provides important insights into the mechanism of binding of four potential inhibitors to the M2 channel of drug-resistant strains of influenza A virus. This

may assist further experimental studies and strategies for rational design of M2 channel inhibitors.

Acknowledgments The work was funded by the Vietnam National Foundation for Science and Technology Development (NAFOSTED), grant number 106.01-2012.66. Computing resources and support provided by the Institute for Computational Science and Technology Ho Chi Minh City are gratefully acknowledged. The authors would like to express their gratitude to Mr Linh Nguyen, Mr Hieu Nguyen, and Mr Thanh Van for valuable advice.

References

Acharya R, Carnevale V, Fiorin G, Levine BG, Polishchuk AL, Balannik V, Samish I, Lamb RA, Pinto LH, DeGrado WF, Klein ML (2010) Structure and mechanism of proton transport through the transmembrane tetrameric M2 protein bundle of the influenza A virus. Proc Natl Acad Sci USA 107:15075–15080

Berendsen HJC, Postma JPM, van Gunsteren WF, DiNola A, Haak JR (1984) Molecular dynamics with coupling to an external bath. J Chem Phys 81:3684–3690

Cady SD, Hong M (2008) Amantadine-induced conformational and dynamical changes of the influenza M2 transmembrane proton channel. Proc Natl Acad Sci USA 105:1483–1488

Cady SD, Schmidt-Rohr K, Wang J, Soto CS, DeGrado WF, Hong M (2010) Structure of the amantadine binding site of influenza M2 proton channels in lipid bilayers. Nature 463:689–692

Darden T, York D, Pedersen L (1993) Particle mesh Ewald: an N-log(N) method for Ewald sums in large systems. J Chem Phys 98:10089–10092

Du Q-S, Huang R-B, Wang S-Q, Chou K-C (2010) Designing inhibitors of M2 proton channel against H1N1 swine influenza virus". PLoS One 5:e9388. doi:10.1371/journal.pone.0009388

Frisch MJ, Trucks GW, Schlegel HB, Scuseria GE, Robb MA, Cheeseman JR, Montgomery JA, Vreven T, Kudin KN, Burant JC, Millam JM, Iyengar SS, Tomasi J, Barone V, Mennucci B, Cossi M, Scalmani G, Rega N, Petersson GA, Nakatsuji H, Hada M, Ehara M, Toyota K, Fukuda R, Hasegawa J, Ishida M, Nakajima T, Honda Y, Kitao O, Nakai H, Klene M, Li X, Knox JE, Hratchian HP, Cross JB, Bakken V, Adamo C, Jaramillo J, Gomperts R, Stratmann RE, Yazyev O, Austin AJ, Cammi R, Pomelli C, Ochterski JM, Ayala PY, Morokuma K, Voth GA, Salvador P, Dannenberg JJ, Zakrzewski VG, Dapprich S, Daniels AD, Strain MC, Farkas O, Malick DK, Rabuck AD, Raghavachari K, Foresman JB, Ortiz JV, Cui Q, Baboul AG, Clifford S, Cioslowski J, Stefanov BB, Liu G, Liashenko A, Piskorz P, Komaromi I, Martin RL, Fox DJ, Keith T, Al-Laham MA, Peng CY, Nanayakkara A, Challacombe M, Gill PMW, Johnson B, Chen W, Wong MW, Gonzalez C, Pople JA (2004) Gaussian 03, revision C.02. Gaussian, Inc., Wallingford

Hay AJ, Wolstenholme AJ, Skehel JJ, Smith MH (1985) The molecular basis of the specific anti-influenza action of amantadine. EMBO J 4:3021–3024

Hess B, Bekker H, Berendsen HJC, Fraaije JGEM (1997) LINCS: a linear constraint solver for molecular simulations. J Comput Chem 18:1463–1472

Hess B, Kutzner C, Spoel DVD, Lindahl E (2008) GROMACS 4: algorithms for highly efficient, load-balanced, and scalable molecular simulation. J Chem Theory Comput 4:435–447

Hockney RW, Goel SP, Eastwood JW (1974) Quit high-resolution computer models of plasma. J Comput Phys 14:148–158

Holsinger LJ, Lamb RA (1991) Influenza virus M2 integral membrane protein is a homotetramer stabilized by formation of disulfide bonds. J Virol 183:32–43

Hu J, Fu R, Nishimura K, Zhang L, Zhou H-X, Busath DD, Vijayvergiya V, Cross TA (2006) Histidines, heart of the hydrogen ion channel from influenza A virus: toward an understanding of conductance and proton selectivity. Proc Natl Acad Sci USA 103:6865–6870

Hu J, Asbury T, Achutha S, Li C, Bertram R, Quine JR, Fu R, Cross TA (2007) Backbone structure of the amantadine-blocked *trans*-membrane domain M2 proton channel from influenza A virus. Biophys J 92:4335–4343

Humphrey W, Dalke A, Schulten K (1996) VMD-visual molecular dynamics. Molecular Graphics. 14:33–38

Jefferson T, Deeks JJ, Demicheli V, Rivetti D, Rudin M (2004) Amantadine and rimantadine for preventing and treating influenza A in adults. Cochrane Database Syst Rev 3:CD001169

Jing X, Ma C, Ohigashi Y, Oliveira FA, Jardetzky TS, Pinto LH, Lamb RA (2008) Functional studies indicate amantadine binds to the pore of the influenza A virus M2 proton-selective ion channel. Proc Natl Acad Sci USA 105:10967–10972

Klösgen B, Helfrich W (1997) Cryo-Transmission Electron Microscopy of a Superstructure of Fluid Dioleoylphosphatidylcholine (DOPC) membranes. Biophys J 73:3016–3020

Kovacs FA, Denny JK, Song Z, Quine JR, Cross TA (2000) Helix tilt of the M2 transmembrane peptide from influenza A virus: an intrinsic property. J Mol Biol 295:117–125

Kukol A, Adams PD, Rice LM, Brunger AT, Arkin TI (1999) Experimentally based orientational refinement of membrane protein models: a structure for the influenza A M2 H^+ channel. J Mol Biol 286:951–962

Lamb RA, Zebedee SL, Richardson CD (1985) Influenza virus M2 protein is an integral membrane protein expressed on the infected-cell surface. Cell 40:627–633

Le L, Leluk J (2011) Study on phylogenetic relationship, variability, and correlated mutations in M2 proteins of influenza virus A. PLoS One 6:e22970. doi:10.1371/journal.pone.0022970

Le L, Lee EH, Hardy DJ, Truong TN, Schulten K (2010) Molecular Dynamics Simulations Suggest that Electrostatic Funnel Directs Binding of Tamiflu to Influenza N1 Neuraminidases. PLoS Comput Biol 6(9):e1000939. doi:10.1371/journal.pcbi.1000939

Lin TI, Schroeder C (2001) Definitive assignment of proton selectivity and attoampere unitary current to the M2 ion channel protein of influenza virus. J Virol 75:3647–3656

Mark P, Nilsson L (2001) Structure and dynamics of the TIP3P, SPC, and SPC/E water models at 298 K. J Phys Chem A 105:9954–9960

Nguyen TT, Mai BK, Li MS (2011) Study of Tamiflu sensitivity to variants of A/H5N1 virus using different force fields. J Chem Inf Model 51:2266–2276

Nishimura K, Kim S, Zhang L, Cross TA (2002) The closed state of a H+ channel helical bundle combining precise orientational and distance restraints from solid state NMR. Biochemistry 41:13170–13177

Ohigashi Y, Ma C, Jing X, Balannick V, Pinto LH, Lamb RA (2009) An amantadine-sensitive chimeric BM2 ion channel of influenza B virus has implications for the mechanism of drug inhibition. Proc Natl Acad Sci USA 106:18775–18779

Okada A, Miura T, Takeuchi H (2001) Protonation of histidine and histidine-tryptophan interaction in the activation of the M2 ion channel from influenza a virus. Biochemistry 40:6053–6060

Parrinello M, Rahman A (1981) Polymorphic transitions in single crystals: a new molecular dynamics method. J Appl Phys 52:7182–7190

Pielak RM, Chou JJ (2010) Flu channel drug resistance: a tale of two sites. Protein Cell 1:246–258

Pinto LH, Holsinger LJ, Lamb RA (1992) Influenza virus M2 protein has ion channel activity. Cell 69:517–528

Roman AL, Swindells MB (2011) LigPlot+: multiple ligand—protein interaction diagrams for drug discovery. J Chem Inf Model 51:2778–2786

Schnell JR, Chou JJ (2008) Structure and mechanism of the M2 proton channel of influenza A virus. Nature 451:591–595

Sharma M, Yi M, Dong H, Qin H, Peterson E, Busath DD, Zhou H-X, Cross TA (2010) Insight into the mechanism of the influenza A proton channel from a structure in a lipid bilayer. Science 330:509–512

Stephenson I, Nicholson KG (2001) Influenza: vaccination and treatment. Eur Respir J 17:1282–1293

Stouffer AL, Acharya R, Salom D, Levine AS, Costanzo LD, Soto CS, Tereshko V, Nanda V, Stayrook S, DeGrado WF (2008) Structural basis for the function and inhibition of an influenza virus proton channel. Nature 451:596–599

Sugrue RJ, Hay AJ (1991) Structural characteristics of the M2 protein of influenza A viruses: evidence that it forms a tetrameric channel. J Virol 180:617–624

Takeda M, Pekosz A, Shuck K, Pinto LH, Lamb RA (2002) Influenza a virus M2 ion channel activity is essential for efficient replication in tissue culture. J Virol 76:1391–1399

Tang Y, Zaitseva F, Lamb RA, Pinto LH (2002) The gate of the influenza virus M_2 proton channel is formed by a single tryptophan residue. J Biol Chem 277:39880–39886

Tian C, Gao PF, Pinto LH, Lamb RA, Cross TA (2003) Initial structural and dynamic characterization of the M2 protein transmembrane and amphipathic helices in lipid bilayers. Protein Sci 12:2597–2605

Tran L, Le L (2014) Recent progress and challenges in the computer-aided design of inhibitors for influenza A M2 channel proteins. Med Chem Res. doi:10.1007/s00044-014-0964-6

Tran L, Choi SB, Al-Naiiar BO, Yusuf M, Wahab HA, Le L (2011) Discovery of potential M2 channel inhibitors based on the amantadine scaffold via virtual screening and pharmacophore modeling. Molecules 16:10227–10255

Tran N, Tran L, Le L (2013) Strategy in structure-based drugs design for influenza A virus targeting M2 channel proteins. Med Chem Res 12:6078–6088

Trott O, Olson AJ (2010) AutoDock Vina: improving the speed and accuracy of docking with a new scoring function, efficient optimization, and multithreading. J Comput Chem 31:455–461

van Gunsteren WF, Billeter SR, Eising AA, Hünenberger PH, Krüger P, Mark AE, Scott WRP, Tironi IG (1996) Biomolecular simulation: the GROMOS96 manual and userguide. Vdf Hochschulverlag AG an der ETH Zurich, Zurich, pp 1–1042

Venkataraman P, Lamb RA, Pinto LH (2005) Chemical rescue of histidine selectivity filter mutants of the M2 ion channel of influenza A virus. J Biol Chem 280:21463–21472

Wallace AC, Laskowski RA, Thornton JM (1995) LIGPLOT: a program to generate schematic diagrams of protein-ligand interactions. J Protein Eng 8:127–134

Wang C, Takeuchi K, Pinto LH, Lamb RA (1993) Ion channel activity of influenza A virus M2 protein: characterization of the amantadine block. J Virol 67:5585–5594

Wang C, Lamb RA, Pinto LH (1995) Activation of the M2 ion channel of influenza virus: a role for the transmembrane domain histidine residue. Biophys J 69:1363–1371

Wang J, Morin P, Wang W, Kollman PA (2001) Use of MM-PBSA in reproducing the binding free energies to HIV-1 RT of TIBO derivatives and predicting the binding mode to HIV-1 RT of efavirenz by docking and MM-PBSA. J Am Chem Soc 123:5221–5230

Yi M, Cross TA, Zhou H-X (2008) A secondary gate as a mechanism for inhibition of the M2 proton channel by amantadine. J Phys Chem B 112:7977–7979